Live Cell Chemical Profiling of Temporal Redox Dynamics in a Photoautotrophic Cyanobacterium

ARTICLE *in* ACS CHEMICAL BIOLOGY · OCTOBER 2013

Impact Factor: 5.33 · DOI: 10.1021/cb400769v · Source: PubMed

14 AUTHORS, INCLUDING:

Margrethe H Serres
Marine Biological Laboratory
28 PUBLICATIONS **1,416** CITATIONS
SEE PROFILE

Eric D Merkley
Pacific Northwest National Laboratory
24 PUBLICATIONS **241** CITATIONS
SEE PROFILE

Richard D Smith
Pacific Northwest National Laboratory
1,131 PUBLICATIONS **45,995** CITATIONS
SEE PROFILE

Aaron T Wright
Pacific Northwest National Laboratory
35 PUBLICATIONS **1,246** CITATIONS
SEE PROFILE

ACS chemical biology

Articles

pubs.acs.org/acschemicalbiology

Live Cell Chemical Profiling of Temporal Redox Dynamics in a Photoautotrophic Cyanobacterium

Natalie C. Sadler,[†] Matthew R. Melnicki,[†] Margrethe H. Serres,[‡] Eric D. Merkley,[†] William B. Chrisler,[†] Eric A. Hill,[†] Margaret F. Romine,[†] Sangtae Kim,[†] Erika M. Zink,[†] Suchitra Datta,[†] Richard D. Smith,[†] Alexander S. Beliaev,[†] Allan Konopka,[†] and Aaron T. Wright*[,†]

[†]Biological Sciences Division, Pacific Northwest National Laboratory, Richland, Washington 99352, United States

[‡]Bay Paul Center, Marine Biological Laboratory, Woods Hole, Massachussetts 02543, United States

Supporting Information

ABSTRACT: Protein reduction−oxidation (redox) modification is an important mechanism that allows microorganisms to sense environmental changes and initiate cellular responses. We have developed a quantitative chemical probe approach for live cell labeling and imaging of proteins that are sensitive to redox modifications. We utilize this *in vivo* strategy to identify 176 proteins undergoing ∼5−10-fold dynamic redox change in response to nutrient limitation and subsequent replenishment in the photoautotrophic cyanobacterium *Synechococcus* sp. PCC 7002. We detect redox changes in as little as 30 s after nutrient perturbation and oscillations in reduction and oxidation for 60 min following the perturbation. Many of the proteins undergoing dynamic redox transformations participate in the major components for the production (photosystems and electron transport chains) or consumption (Calvin−Benson cycle and protein synthesis) of reductant and/or energy in photosynthetic organisms. Thus, our *in vivo* approach reveals new redox-susceptible proteins and validates those previously identified *in vitro*.

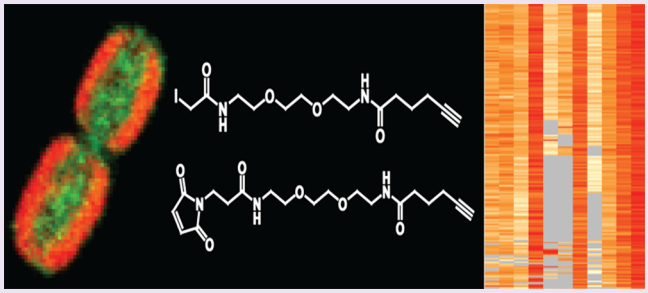

Photoautotrophic organisms maximize light energy utilization efficiencies through balancing the rates of reductant generation and consumption. They must also regulate the intracellular redox environment by responding to reactive oxygen species (ROS) that arise as a consequence of photosynthesis.[1] *In vivo* redox control is postulated to be an important acclimation mechanism of microorganisms to environmental variations, implying both perception of change and initiation of cellular responses.[2] Redox sensing involves multiple layers of cellular machinery in which electron transport systems supply electrons to redox input elements such as ferredoxin, reduced NAD(P)H, and glutathione. These elements donate electrons to redox transmitters (*e.g.*, thioredoxins and glutaredoxins) that subsequently alter the redox state of target proteins *via* reactions with cysteine residues,[3] affecting important processes in the cell.[4−6] Understanding photoautotrophic redox control of proteins, particularly those pertinent to the generation of reductants, protein and/or biomass synthesis and carbon flux through central metabolic pathways, may yield targets for creating metabolically optimized microorganisms for bioenergy production.

From a mechanistic standpoint, cysteine represents a critical redox-responsive amino acid within proteins, largely due to the range of sulfur oxidation states. The reversible reduction and oxidation of paired inter- and intraprotein cysteine residues, or paired cysteine residues and small molecules (*e.g.*, glutathione), in selected proteins is known as cysteine thiol-disulfide exchange (CTDE)[7−11] and is thought to be a particularly important means of regulating protein function and signal transduction.[4,12−14] However, the lack of a recognizable conserved motif that confers protein susceptibility to redox sensitivity makes their systematic identification difficult.[15] Proteomic screening methods using column trapping or gel electrophoresis of reduced dithiols after *in vitro* reduction of lysates have been exploited to identify redox-sensitive proteins.[8] Yet these techniques can only identify candidates for potential redox-susceptible proteins, as cell lysis disturbs the native context, disrupting or destroying sensitive modifications and thereby producing artifacts.[8,11] Herein, we will demonstrate a chemical probe approach that overcomes these obstacles by direct *in vivo* measurement of proteins participating in redox events.

Live cell measurement of dynamic redox events involving cysteine residues in proteins is desirable because (i) change in redox status often occurs on short time scales concurrent with environmental (*i.e.*, irradiance, O_2 concentration, nutrient) changes,[16] (ii) cell lysis promotes rapid oxidation, creating artifacts,[11,17−19] and (iii) redox modification of cysteines often depends on subcellular localization, orientation, and topology.[4]

Received: July 16, 2013
Accepted: October 29, 2013
Published: October 29, 2013

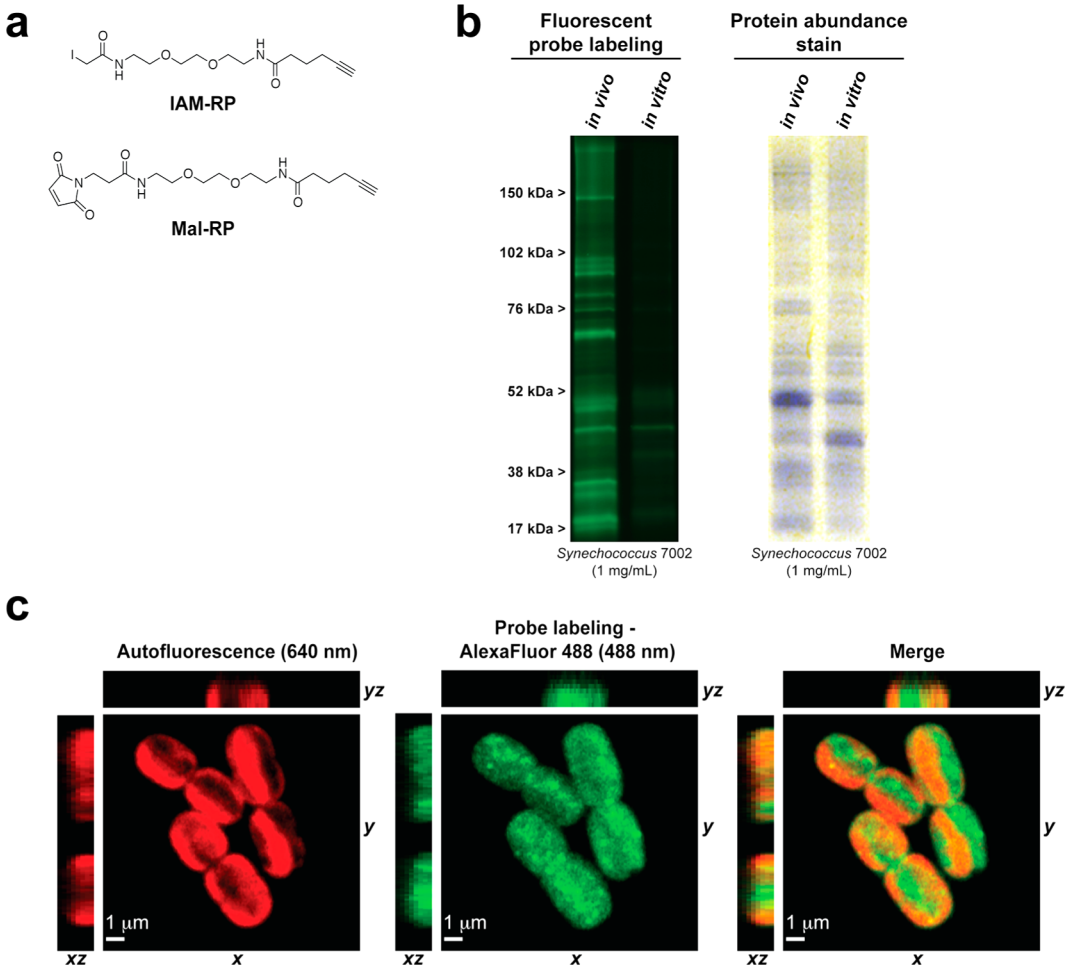

Figure 1. Chemical probes for *in vivo* labeling of reduced cysteine thiols. (a) **IAM-RP** and **Mal-RP**. (b) *In vivo* (whole cell) versus *in vitro* (cell lysate) labeling of *Synechococcus* 7002. Proteins were separated by SDS-PAGE and imaged either by labeling with fluorescent probes (left panel; tetramethylrhodamine-azide added by click chemistry) or Coomassie Blue staining for total protein abundance (right panel). (c) Laser-scanning confocal microscopy of *in vivo* probe-labeled *Synechococcus* 7002 cells imaged either from autofluorescence of phycobilisomes associated with photosynthetic membranes (left) or AlexaFluor-488 bound to chemical probe-labeled proteins (center). The right panel displays the merged image. On the left of each panel is the *XZ*-plane image, and on top of each panel is the *YZ*-plane image, permitting a 3D view into the center of the cells. See Supplementary Figure 1 for control images and the Supplementary Video for a rotational 3D movie showing *in vivo* labeling.

Present methods attempt to preserve the redox status of cysteine thiols by adding trichloroacetic acid during cell lysis;[20] however, this may cause protein denaturation, disrupting the structural context of labeling sites, without fully preserving the functional context of the cellular environment.[21]

In this study we report the development and application of thiol-targeting chemical probes *in vivo* to the photoautotrophic cyanobacterium *Synechococcus* sp. PCC 7002 (hereafter, *Synechococcus* 7002). In order to create a biological platform with a disruption in available cellular reductant, we limited and then starved *Synechococcus* 7002 of a carbon source. Being that CO_2 availability is known to affect photosynthetic energy transduction, both directly as a cofactor in PSII and indirectly *via* disruption of homeostasis of the Calvin–Benson cycle,[22] the major sink for ATP and reductant,[23] a C-perturbed environment will result in protein labeling variability as cysteine thiols undergo redox in response to fluctuations in carbon, reductant, and ATP.

We identify a temporal continuum of dynamic cyclic redox fluctuations of cysteine thiols after a shift from C-starvation to replenishment and measure redox changes over time spans of seconds to minutes in 176 proteins with ~5–10-fold dynamic range; by LC–MS we also identify the specific probe-labeled cysteine(s) in 106 of the 176 identified proteins. Additionally, microscopic imaging was used to visualize probe labeling within live cells. Our results reveal a series of newly identified proteins that undergo dynamic redox changes and potentially govern a wide range of biological processes including signal transduction, ROS remediation, photosynthesis, metabolism, and protein synthesis.

RESULTS AND DISCUSSION

Development and Validation of Chemical Probes for Quantitative Characterization of Protein Redox. To elucidate redox-sensitive proteins both *in vitro* and *in vivo*, we designed and synthesized two cysteine thiol-specific redox probes (RP). The developed probes (Figure 1a) share three key features that enable quantitative analysis of protein thiol redox in living cells: (i) an electrophilic group derived from either iodoacetamide (**IAM-RP**) or *N*-ethylmaleimide (**Mal-RP**) to covalently label the reduced thiol form of cysteines;[13,24,25] (ii) ethylene glycol spacers, which impart cell permeability;[26] and (iii) an alkyne handle, for 'click chemistry' conjugation to a functionalized group for fluorescent detection and/or enrich-

dx.doi.org/10.1021/cb400769v | *ACS Chem. Biol.* 2014, 9, 291–300

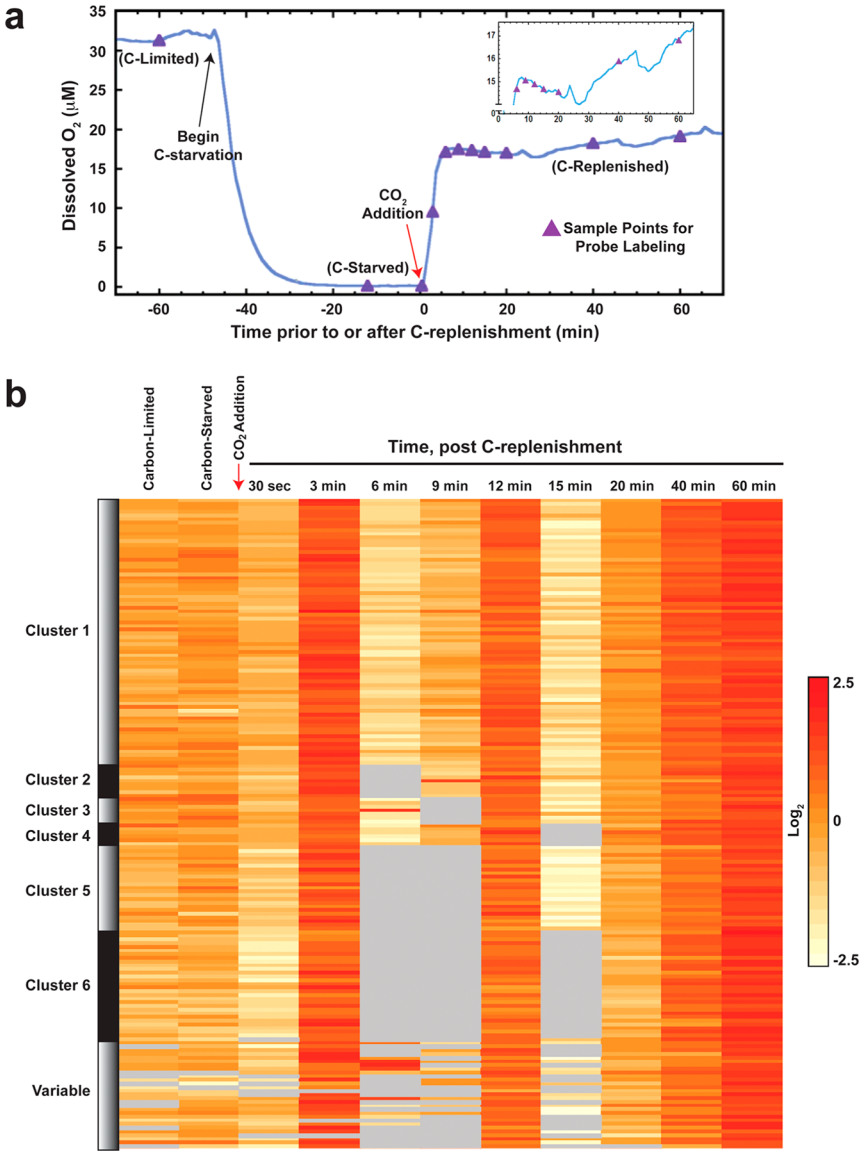

Figure 2. Effects of CO_2 replenishment upon redox status of proteins in live *Synechococcus* 7002 cells. (a) Changes in photosynthetic activity (inferred from dissolved O_2 concentrations) as CO_2 availability was manipulated (limitation, starvation, and replenishment). Triangles indicate times when samples were taken for *in vivo* probe labeling. The inset highlights the 6–60 min region, showing fluctuations in the dissolved O_2 concentration. (b) Temporal changes of *in vivo* labeling with **IAM**- and **Mal-RPs** in 176 proteins. The proteins were grouped by K-means clustering of Euclidean distance based upon the temporal dynamics in probe labeling. The heat map portrays times when specific proteins are most reduced (red) versus more oxidized (light yellow). Gray coloring indicates that oxidation is so significant that no detectable probe labeling was observed. The color range represents 2^5-fold difference in probe labeling. The numerical changes for proteins are listed in Supplementary Data Set 3, as are the specific cysteine residues labeled by the probe. Data in the heatmap represents three replicates at each time point.

ment followed by LC–MS.[27] The alkyne group also prevents hindrance of binding and increases permeability while permitting flexibility of functionalization. Enriched probe labeled proteins were quantitatively measured by LC–MS using the accurate mass and time (AMT) tag approach.[28]

Both **IAM**- and **Mal-RPs** were verified to detect redox-sensitive proteins *in vitro*, using cell lysates from *Synechococcus* 7002. Cysteine thiols not participating in disulfide bonds were first "blocked" by alkylation with iodoacetamide and *N*-ethylmaleimide, followed by reduction of cysteine disulfides with tris(2-carboxyethyl)phosphine (TCEP) and probe labeling of the TCEP-reduced cysteines. Upon subsequent enrichment and LC–MS analysis, we identified 186 and 209 proteins labeled by **IAM-RP** and **Mal-RP**, respectively, with 182 of these proteins detected by both probes (Supplementary Data Set 1). While this overlap suggests that the two probes share a high degree of target specificity, quantitative AMT analysis indicates differing reactivity. Beyond the 10 most abundantly labeled proteins, which react similarly with both probes, the order of reactivity based upon observed abundances is highly variable. Accordingly, *N*-ethylmaleimide has previously been shown to be a stronger alkylating agent than iodoacetamide toward extrinsic thiols, whereas iodoacetamide is more reactive than *N*-ethylmaleimide toward buried or partially exposed thiols.[29] Thus, to maximize detection, we employed a combination of both **IAM-RP** and **Mal-RP** for *in vivo* labeling studies.

In vitro probe labeling in *Synechococcus* 7002 was also performed using a pretreatment with recombinant thioredoxin from *E. coli* (TrxA) to simulate the mechanism of disulfide reduction by a native electron donor. *In vivo*, thioredoxin (Trx)

dx.doi.org/10.1021/cb400769v | *ACS Chem. Biol.* 2014, 9, 291–300

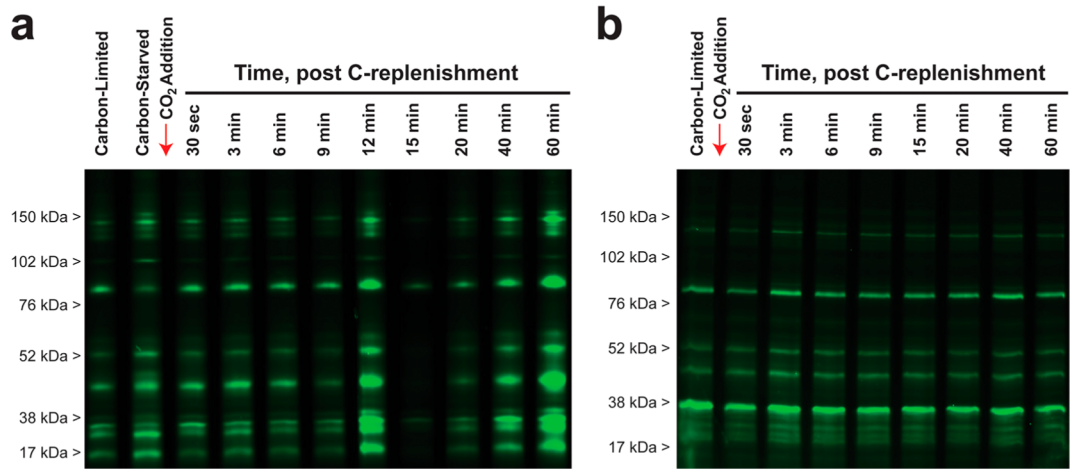

Figure 3. IAM-RP and **Mal-RP** *in vivo* labeled samples. Following labeling cells were lysed and appended to a fluorophore by CuAAC, and then proteins were separated by SDS-PAGE and imaged. (a) *Synechococcus* 7002 was transitioned from a C-limited steady state to a C-starved state, and then C was replenished over a 60 min time course. (b) *Synechococcus* 7002 was transitioned directly from a C-limited steady state to C-replenished over a 60 min time course (see also Supplementary Figure S2 for protein abundance stains).

acts as a redox transmitter by reducing disulfides in oxidized target proteins *via* CTDE, affecting important processes in the cell.[4,6] Here, *Synechococcus* 7002 lysates were alkylated with iodoacetamide and *N*-ethylmaleimide to alkylate thiols not involved in redox reactions, then reduced with Trx, and subsequently probed with **IAM-RP**, resulting in 76 labeled proteins (Supplementary Data Set 2). The lower diversity of labeled proteins with TrxA could have several potential explanations: the use of a single subtype of a non-native Trx, expenditure of reducing capacity, Trx preference for intramolecular disulfides, thioredoxin's susceptibility to aerobic oxidation in *in vitro* conditions, or glutathionylation of cysteine residues.[4] Additionally, the subset of redox-sensitive proteins we identify here are specific to our growth conditions. In both the TCEP and TrxA studies we used no probe and no added reducing agent controls to minimize potential false positives. However, 35 of the 76 labeled proteins have been previously identified in another well-studied cyanobacterium, *Synechocystis* sp. PCC 6803, revealing our approach's capability to both confirm and reveal new identifications (Supplementary Data Set 3).[7,11]

Application of Mal-RP and IAM-RP for *in Vivo* Labeling: Fluorescent Imaging. The cell-permeable **Mal-RP** and **IAM-RP** probes were applied to live *Synechococcus* 7002 cells to trap intracellular redox-sensitive cysteines in their reduced state. When equivalent protein concentrations were compared by SDS gel electrophoresis (Figure 1b) *in vivo* labeling was much greater than that of *in vitro*, confirming prior reports that cell lysis induces cysteine oxidation and lending credence to the need for an *in vivo* approach.

To demonstrate that the probes are cell permeable and enter live cells, **Mal-RP** and **IAM-RP** were applied *in vivo* to *Synechococcus* 7002, followed by addition of AlexaFluor-488. Laser-scanning confocal microscopy with Z-stacking was used to three-dimensionally image either autofluorescence of phycobilisomes associated with photosynthetic membranes at 640 nm (Figure 1c, left panel) or probe-labeled proteins *via* AlexaFluor fluorescence at 488 nm (Figure 1c, center panel). The merged image (Figure 1c, right panel) illustrates relative probe labeling in the membranes and cytosol (Figure 1c, right panel; see also Supplementary Figure 1). Figure 1c also shows the *XY*- and *YZ*-planes, providing three-dimensional clarity demonstrating probe labeling and cytosol/membrane distribution within the cells (see also the Supplementary Video). Although low molecular weight thiol-containing compounds could be labeled, the pattern of punctate probe localization within the cytosol (Figure 1c, center and right panels; Supplementary Video) suggests labeling of localized protein complexes, *e.g.*, carboxysomes that contain highly abundant RuBisCO- a critical enzyme for C-fixation.

Live Cell Identification of a Temporal Continuum of Protein Redox Dynamics in *Synechococcus* 7002 in Response to Carbon Replenishment. The redox state of protein thiols should be sensitive to sinks for reductant generated *via* photosynthesis. Therefore, we imposed a large perturbation in the major sink for reductant (CO_2 fixation *via* the Calvin–Benson cycle) by depriving a steady-state C-limited continuous culture of CO_2 inputs for 48 min (C-starvation). $CO_{2(g)}$ was then supplied by the sparging gas (C-replenishment phase). Photosynthetic O_2 evolution rapidly resumed (Figure 2a) after C-replenishment; cells were probe-labeled at nine time points over the next 60 min. Significant decreases in probe labeling, indicating widespread protein oxidation, were observed 30 s after C-replenishment (Figures 2b and 3a and Supplementary Data Set 3). At 3 min post C-replenishment, increased probe labeling was observed indicating the reduction of thiols. Thereafter, the pattern of redox labeling exhibited temporal cycles, characterized by significant shifts between reduced and oxidized proteoforms (Figure 2b and 3a). When C was replenished light energy harvesting rates, reductant and ATP production, and carbon fixation all needed to recalibrate to establish appropriate stoichiometric rates for homeostasis. It was previously reported that when photoautotrophs transition from a low to high C condition, photosynthetic rates oscillate because of the imbalances in the availability of ATP and NADPH for carbon reduction.[23]

To validate these results, we performed a second experiment in which C was directly replenished in C-limited steady state *Synechococcus* 7002 cells and probe-sampled *in vivo* over 60 min (Figure 3b). In contrast to the first experiment, C addition to a C-limited steady state is a minor perturbation. The redox oscillations in the C-limited experiment were found to be minor

dx.doi.org/10.1021/cb400769v | *ACS Chem. Biol.* 2014, 9, 291–300

compared to C replenishment of C-starved cells (Figure 3). These experiments establish that our *in vivo* probe approach is highly sensitive to redox dynamics and demonstrate that the probes do not themselves create an artifactual cellular response.

Data analysis of the global proteome revealed 808 proteins across all sampling time points of the C-replenishment experiment. Importantly, no significant differences in protein abundance were measured for the global proteome across all time points (Supplementary Figure 3; Supplementary Data Set 4), thus underscoring that the cycled pattern of labeling reflects redox modifications that affect probe reactivity and not protein abundance variability between samples. Of the 176 probe-identified proteins, 166 were also identified in the global analysis. This suggests that differences in detection across time points in the probe-labeled proteomes are not merely a statistical consequence of inadequate proteome coverage. In fact, the simplified proteome pulled down by the probe would be less susceptible to missing proteome coverage than the global proteome due to the smaller subset of peptides being analyzed.

Of the 808 proteins detected by global proteome analysis, 687 contain one or more cysteines. The thiol probes did not indiscriminately label all cysteines in proteins, as only 176 proteins were detected in the set of samples treated with the probes. The temporal dynamics in relative probe labeling for this restricted set of cysteine-containing proteins indicate that the probes detect reversible changes of cysteine redox status or structural changes affecting thiol accessibility in redox susceptible proteins. For ~60% of these 176 proteins, we have identified the specific probe-labeled cysteine residue (Supplementary Data Set 3), revealing these sites for the first time for cyanobacterial proteins. To rule out potential off-target probe labeling, we also searched for probe modification of other residues such as Tyr, His, Lys, and Met and found none.

The redox response of protein thiols during C-replenishment was compared to changes in photophysiology at similar time points, using pulse amplitude modulated (PAM) fluorometry to measure changes of the variable chlorophyll fluorescence that directly correspond to the redox status of the primary quinone electron acceptor (Q_A) within PSII. Based on this relationship, particular manipulations of sample illumination induce fluorescence dynamics that reveal information about PSII functionality, as well as electron transport processes "downstream" from the primary water-splitting reaction at PSII.

Upon C-starvation, a 25% decline in the photosystem II (PSII) quantum yield (Y_{II}) was observed, but Y_{II} recovered within 30 s after supplying CO_2 (Figure 4a). Photochemical quenching (qP) responded similarly, reflecting an increased proportion of functional PSII. While these values remained high between 0 and 12 min, a transient spike in the rate of cyclic electron flow (CEF) was observed (Figure 4a), indicating feedback of reductant from NAD(P)H into the plastoquinone (PQ) pool. This suggests that electron transport downstream of photosynthesis was impaired during C-starvation, and is supported by the delayed recovery of the rate of dark PQ reoxidation and the gradual restoration of P≫S quenching, which is influenced by downstream processes (Figure 4b). During this early phase, metabolic processes were incapable of consuming reductant fast enough to accommodate the abrupt restoration of PSII activity. A second phase of recovery was observed 20−60 min after supplying CO_2, in which Y_{II} and qP maintained lower levels while CEF and PQ reoxidation rates rose together, establishing stable values from 40 to 60 min.

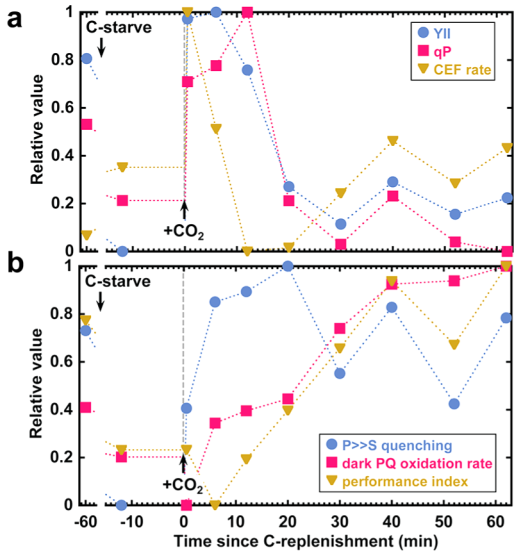

Figure 4. Effects of CO_2 replenishment upon the status of photosynthetic electron flow in live *Synechococcus* 7002 cells. Chlorophyll fluorescence induction, saturation pulse, and postillumination kinetics were recorded by PAM fluorometry and plotted as relative changes over the course of the experiment. Samples were obtained from the CO_2-limited chemostat (−60 min), after 48 min of C-starvation (−12 min), and throughout the timecourse after C-replenishment (0.5, 6, 12, 20, 30, 40, 52, 62 min). For each parameter, the minimum and maximum values are presented in parentheses. (a) PSII quantum yield (Y_{II}): (0.192, 0.262); photochemical quenching (qP) (0.628, 0.865); relative rate of NAD(P)H-based cyclic electron flow (CEF) (0.00320, 0.00741). (b) Relative rate of downstream electron transport (P ≫ S quenching) (0.034, 0.240); postillumination relaxation slope (dark PQ oxidation rate) (2.69×10^{-4},8.24×10^{-4}); performance index on absorption basis (0, 6.66×10^{-3}).

These values suggest that metabolic electron sinks (*e.g.*, carbon fixation) were consuming reductant at a rate commensurate with its generation. The two cycles of protein oxidation and rereduction detected by probe labeling during the first 12 min may be related to the unbalanced production of ROS and reductant as electron transport processes re-equilibrate. We hypothesize that the regulatory effects of oxidation and reduction upon protein activity aid in establishing a more balanced metabolic state after 20 min, as seen from the Performance Index (Figure 4b). This parameter will attain higher values only when each element of the photosynthetic apparatus is operating at rates in concert with the others.[30] Finally, it is not surprising that the redox dynamics were dissimilar between the 60 min time point and the original C-limited steady state, as the 60 min time point represents a transition phase toward a new C-replete steady state.

Temporal Cycles of Redox Modification After Carbon-Replenishment. Cluster analysis of probe labeling revealed six distinct temporal trends dominated by 72 proteins in cluster 1 that displayed <10-fold changes between reduced and oxidized proteoforms (Figure 2b; clusters are in Supplementary Data Set 3). The other five clusters contain proteins that were undetectable by probe labeling in at least one time point, likely indicative of complete oxidation. Outliers from the general trends include proteins that experience redox chemistry *via* alternative mechanisms, *e.g.* glutaredoxin and a putative DsbAB. Glutaredoxin reduces glutathione-protein adducts, while DsbAB is responsible for oxidizing protein substrates in the cytoplasm. All 176 identified proteins fluctuated in their

dx.doi.org/10.1021/cb400769v | *ACS Chem. Biol.* 2014, 9, 291−300

levels of probe labeling over a function of time indicating their altered redox status. The oscillatory effects observed are not surprising because physiologically the cells utilize regulatory mechanisms to attempt to maintain homeostasis between reductant generation and consumption.

Characterization of Live Cell Probe-Labeled Proteins Reveals Broad Control of Metabolic Subsystems. By grouping the dynamically labeled proteins by putative function or pathway classification (Table 1), it is apparent that newly

Table 1. Biological Processes and Pathways Represented by Live-Cell Probe-Labeled Proteins Identified during C-Replenishment in *Synechococcus* 7002[a] and prior IDs in *Synechocystis* 6803 and *Arabidopsis*

function	7002	6803	*Arabidopsis*	new IDs
photosynthesis	23	7	6	10
electron transport/ATP synthesis	10	2	5	5
CO_2 fixation	14	8	10	3
intermediary metabolism	9	5	3	4
biosynthesis	45	9	9	31
redox regulators	10	3	4	5
transcription/regulation	12	4	0	8
translation	27	10	8	13
misc	26	3	1	22
totals	176	51	46	101

[a]See Supplementary Data Set 3 for protein assignments.

detected redox-sensitive proteins were members of all major metabolic systems. These groupings are consistent with enrichment of selected pathways and gene ontology biological processes (Supplementary Data Sets 5 and 6). Of 176 probe labeled proteins, 101 are newly identified as redox-sensitive, while the remaining 75 have been previously found as regulated by Trx or susceptible to CTDE in cyanobacteria (*Synechocystis* 6803) or plants (*Arabidopsis thaliana*) (Table 1 and Supplementary Data Set 3).

When this catalog of proteins was compared to those detected during *in vitro* Trx- and TCEP-reduced experiments (Supplementary Figure 4a), 59 proteins were common to all three, and 100 proteins detected *in vivo* were also observed using one of the two *in vitro* methods. These discrepancies may result from artifacts during the sample processing or physiological differences between the cells used in these experiments.

Subcellular localization analysis revealed that ~21% of the detected proteins are predicted to be membrane-associated (Supplementary Figure 4b), suggesting that the probes were able to access a variety of cellular compartments *in vivo*. This is highly consistent with the confocal laser-scanning microscopy imaging analyses, in which approximately 20−25% of binding is visualized in the membranes (Figure 1c).

The two photosystems (I and II) and associated electron transport proteins and soluble carriers constitute the machinery whereby reductant (and energy) is conserved in oxygenic phototrophs. While 12 of the 20 proteins required for PSII contain cysteines,[31] only four were labeled *in vivo* (Figure 5a). In contrast, 7 of 11 PSI proteins were labeled (Figure 5b).[8] There were 8 out of 13 phycobilisome antenna complex proteins detected (Figure 5a). Additionally, we labeled two proteins, OcpA and IsiA, postulated to assist in photoprotection under stress.[32]

Novel electron transport proteins detected by *in vivo* probe labeling include the cytochrome b_6 protein PetB; three proteins in the NADH dehydrogenase complex (NdhH, NdhK, NdhN), which may participate in cyclic photosynthetic electron transfer; and flavodoxin (IsiB) (Figure 5c). Although it was previously only detected in plants, the electron transport intermediary FNR (Ferredoxin:NADP+ reductase; PetH) was also revealed by probes. We identified AtpA, AtpD, AtpH, and AtpG subunits of ATP synthase (Figure 5d), consistent with prior observations.[8] It is clear by probe labeling that the redox regulation of multiple protein subunits appears to reflect complicated fine-tuning mechanisms involved in cellular processes.

Importantly, three proteins were labeled that are predicted to be localized within carboxysomes, proteinaceous microcompartments in many CO_2-fixing bacteria.[33] These include two ribulose-1,5-bisphosphate carboxylase-oxygenase (RuBisCo) subunits responsible for CO_2 fixation; two structural proteins, CcmM and CcmK4; and additionally, CupA, a distal membrane subunit of type-1 NAD(P)H dehydrogenase complex associated with CO_2 uptake. Among the 11 enzymes of the Calvin−Benson cycle, which were previously identified as redox-regulated in plants,[34] our measurements yield only 9 enzymes in *Synechococcus* 7002 (Figure 5e and Supplementary Figure 5); labeling was not detected in our live cell experiment or previously in *Synechocystis* 6803[11] for triose-phosphate isomerase (which lacks cysteines) or ribose 5-phosphate isomerase.

Labeling was also detected for the aconitase and citrate synthase enzymes, which catalyze adjacent steps in the TCA pathway; no TCA cycle enzymes were reported from the disulfide proteome of *Synechocystis* 6803. Labeling of both glycogen synthase and glycogen phosphorylase was detected, analogous to redox control of starch synthesis in plants.[35] Biosynthetic pathways in *Synechococcus* 7002 were also redox-sensitive and include proteins involved in amino acid, purine/pyrimidine, and fatty acid biosynthesis (Supplementary Data Set 3).[11]

Proteins Involved in Transcription and Translation Alter Redox Status. Five transcriptional regulators (Table 2) and proteins essential for gene transcription and translation were probe-identified. No transcriptional regulators have been identified previously as redox-sensitive or Trx targets in cyanobacteria. We labeled RbcR, which regulates the transcription of the *rbcLXS* operon encoding the primary carboxylating enzyme for CO_2 fixation, RuBisCO. Two other identified regulators, Fur and Zur, are involved in iron and zinc homeostasis, respectively.[36,37] The regulator CalA is believed to be involved in regulation of C and N metabolism.[38] No function has been associated with the remaining regulator. This is a key finding of this study because it indicates that dynamic redox modulation of protein cysteines may involve not only catalytic enzymes but also gene expression in phototrophs.

Proteins Mediating Redox Signal Transduction. Our probes also detected redox-transmitting proteins that included *y*-type thioredoxin M (TrxQ), *x*-type thioredoxin (TrxB), *m*-type thioredoxin (TrxA), glutaredoxin (GrxB), and thioredoxin dependent peroxiredoxins from the 1-Cys protein family (Prx-1-Cys) and from the PrxII family (PrxII) (Figure 5F).[8] Additionally, we labeled one of the five *Synechococcus* 7002 cyclophilin peptidyl-prolyl cis-trans isomerases, a Trx regulated enzyme linked to photosynthetic electron transport and regulation of chaperones in response to light and oxidative stress in *Arabidopsis* and reduction of peroxiredoxins.[41,42]

dx.doi.org/10.1021/cb400769v | *ACS Chem. Biol.* 2014, 9, 291−300

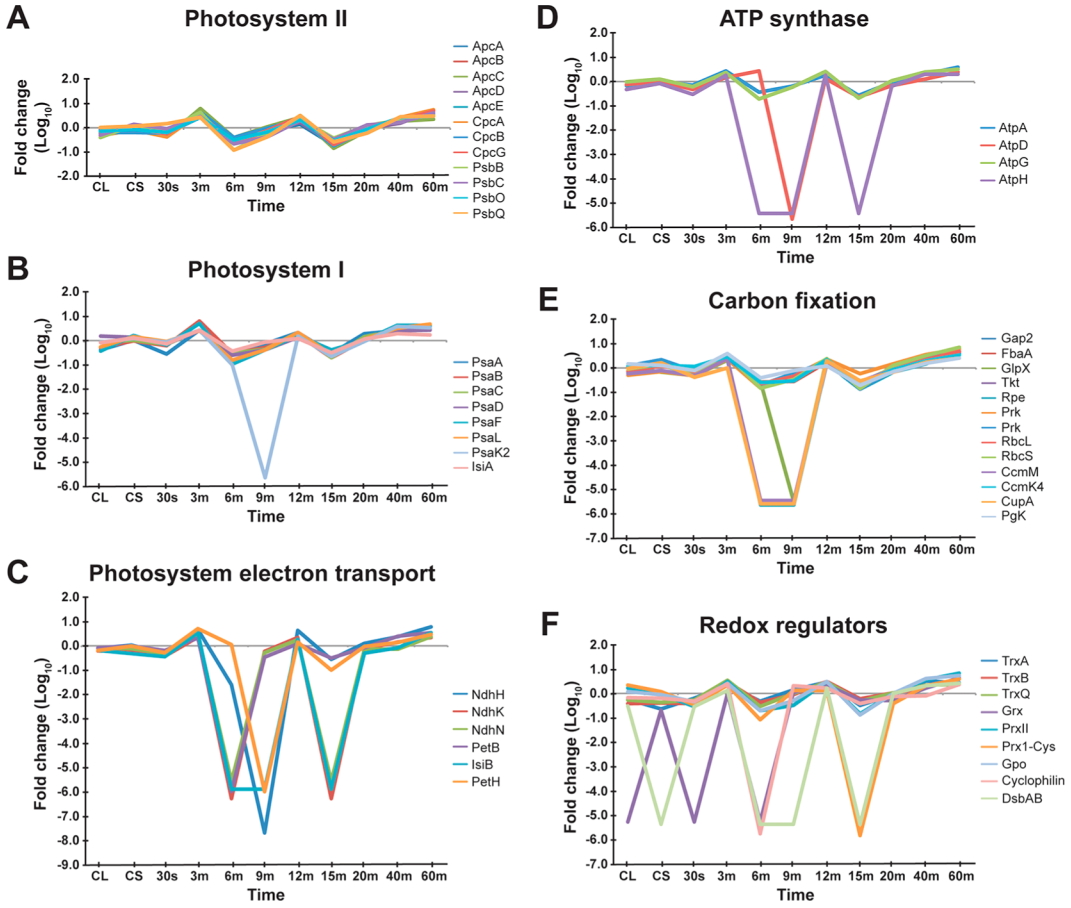

Figure 5. Temporal patterns in redox status of proteins in six functional pathways before and after C-replenishment. Changes in redox status were calculated from the average AMT tag abundance for each protein across three replicates for each time and across all time points, then by calculating the deviation (log_{10}) at each time point from the average across all time points. The largest decreases indicate that the probe did not label that protein (presumably full oxidation). (a) Phycobilisome and photosystem II (PSII). (b) Photosystem I (PSI). (c) Photosystem electron transport. (d) ATP synthases. (e) Carbon fixation. (f) Redox regulators.

Table 2. Redox Regulation of Transcriptional Regulators

locus	regulator	regulated functions[a]
SYNPCC7002_A1095	ArbB family regulator, CalA	C, N metabolism[b]
SYNPCC7002_A1649	Fur family regulator, Fur	iron homeostasis regulon[c]
SYNPCC7002_A1198	LysR family regulator, RbcR	carbon fixation, photorespiration[d]
SYNPCC7002_A2498	Fur family regulator, Zur	zinc homeostasis regulon[e]
SYNPCC7002_A2441	TetR family regulator	not determined

[a]Reference 39. [b]Reference 40. [c]Regulon with 17 operons encoding siderophore and iron receptors/transporters, vitamin B12 transporter, protoporphyrin IX chetalase subunit, pyruvate-flavodoxin oxidoreductase, allophycocyanin subunit, photosystem I P700 chlorophyll a apoproteins A and B, light-independent protochlorophyllide reductase subunits, outer membrane transport energizing system, two-component regulator, and transcriptional regulators. [d]Ribulose bisphosphate carboxylase subunits, chaperone. [e]Regulon with three operons encoding delta-aminolevulinic acid dehydratase, GTP cyclohydrolase, zinc transport, and a transcriptional regulator.

Interestingly, a putative DsbAB bifunctional protein disulfide isomerase/oxidoreductase demonstrated temporal dynamics after CO_2 replenishment.

CONCLUSION

We have used a quantitative live cell probe labeling approach to reveal widespread temporal redox dynamics in the photoautotrophic cyanobacteria *Synechococcus* 7002. Live cell labeling across time permits "titration" of the physiological redox state of the cell and facilitates the dissection of regulatory control across metabolic networks while facilitating an array of research possibilities to measure the dynamic interactions between photosynthetic outputs (reductants) and activity of proteins in cyanobacteria and other photosynthetic organisms. The dynamic modulation of redox that we observed throughout metabolic subsystems (Table 1) suggests a system-wide importance of redox control in balancing the rate of reductant production with its consumption. Additionally, our comparative analysis between resupplying C to both C-starved and C-limited cells demonstrates that the probes report on physiological phenomena, without inducing significant alterations to cellular redox.

The oscillations of protein probe labeling over the C-starved to C-replenished time course suggests that the identified cysteine modifications occurring are in fact reversible redox changes, precluding a significant role for other forms of cysteine thiol modifications such as acylation. This conclusion is also strengthened by the global proteome measurements that showed no significant alterations in protein abundance

dx.doi.org/10.1021/cb400769v | *ACS Chem. Biol.* 2014, 9, 291−300

throughout the duration of the 60 min experiment; therefore, the probe labeling results representative redox alterations and not protein abundance.

Our photophysiology analyses were consistent with our hypothesis that the perturbation generated by CO_2 supply after C-starvation can result in a series of successive metabolic bottlenecks, because nutrient-limitations generally cause an over-reduction of electron transport pools due to metabolic imbalances downstream of photosynthesis.[43] For instance, when NADPH is contributing electrons to downstream metabolic processes such as the Calvin–Benson cycle, elevated cyclic electron flow around PSI may ensue (Figure 4a).[44] However, when electron bottlenecks occur, the consequence is oscillatory physiological parameters, as observed in redox with *in vivo* probing. Theoretical studies have indicated that when cellular regulatory mechanisms have been selected to respond rapidly,[45] the system becomes susceptible to overshoots. Herein, we applied an extreme perturbation, relief of C-starvation, which is more likely to generate oscillations as the regulatory system tries to restore homeostasis than a subtle perturbation, such as a shift from C-limited growth to C-replenished growth (Figure 3). However, it is important to note that system balance, as depicted by the performance index, began to improve 20 min after supplying CO_2. There were also clusters of proteins that exhibited similar patterns of redox dynamics to the performance index after the perturbation (Figure 4b); this suggests rapid temporal effects upon the status of redox transmitters, such as thioredoxin. We infer that regulation *via* these redox transmitters is essential for the re-establishment of metabolic balance.

Redox regulation of metabolic processes in photosynthetic organisms has been investigated for over 50 years.[46] Our approach is complementary to but also extends beyond the biochemical and proteomic studies previously performed *in vitro*. Our method utilizes a chemical tool to monitor reversible redox reactions by capturing reduced cysteines in live cells and will allow for advances in systems biology by creating an illustrative map of the dynamic reversible cysteine reactions associated with protein signaling, regulation, and activity. Additionally, this approach is broadly applicable to investigate redox modulation beyond the organism and conditions defined herein; we have only begun to investigate the diversity and magnitude of redox-regulated CTDE in other prokaryotic and eukaryotic organisms.

METHODS

Probe Synthesis. See the Supporting Information.

***In Vitro* Probe Labeling.** *Synechococcus* 7002 cells were lysed under aerobic conditions *via* bead beating, and protein concentrations were determined for the lysate. The lysates were then alkylated with iodoacetamide (IAM) and *N*-ethylmaleimide (NEM) and treated in one of the following two ways: [A] Alkylated cell lysates were treated with TCEP (250 μM) and incubated at 37 °C for 30 min. Excess reductant was removed by filtration with PBS 3×. The alkylated and reduced cell lysates (1 mg mL^{-1} protein) were treated with **IAM-RP** (20 μM) or **Mal-RP** (5 μM) or DMSO (no probe control) and incubated for 1 h at 37 °C. [B] Alkylated cell lysates (1 mg mL^{-1} protein) were treated with NADPH (1.25 mM), *E. coli* thioredoxin reductase (1.05 μM; Sigma), and *E. coli* TrxA (1.05 μM; Sigma). The alkylated and reduced cell lysates were treated with **IAM-RP** (20 μM) or DMSO. Samples were incubated for 1 h at 37 °C with moderate shaking. For protocols [A] and [B] biotin-azide was added *via* click chemistry.[47] See the Supporting Information for additional details on cell cultivation and extract preparation.

Photobioreactor Cultivation and *in Vivo* Probe Measurements of C-Replenishment. Cells were grown in a custom photobioreactor (see Supporting Information). Upon reaching C-limited steady state (OD_{730} = 0.39), C-starvation was imposed by halting the media delivery for 48 min, followed by C-replenishment by simultaneously restoring media delivery and sparging with 5% CO_2 in N_2 at 4.2 L/min. The C-starvation step was omitted for the C-limited to C-replenished experiment, but all other parameters were consistent. Whole cells in A+ media (35 mL) from the bioreactor were purged from the photobioreactor into prechilled (−10 °C) collection flasks. Cells were pelleted in a rapid 1 min spin, and the media decanted. Three samples were labeled for each sampling time (Figure 2A). To each flask was added 1 mL of PBS containing **Mal-RP** (60 μM) and **IAM-RP** (60 μM). This probe concentration obviates potential labeling of low molecular weight cytosolic thiols such as glutathione or free cysteine; on a mole basis we approximate a 3–5-fold excess of probe to low molecular weight thiol-containing compounds. Following probe labeling, samples were incubated for 30 min, pelleted, washed 4× with PBS, and lysed at 0 °C using a Bullet Blender (power setting 8). Biotin-azide was added *via* click chemistry.[47]

Fluorescent Gel Imaging of *in Vitro* versus *in Vivo* Probe Labeling. *Synechococcus* 7002 cells cultivated in a photobioreactor (OD = 0.08) were collected (50 mL). *In vivo* and *in vitro* probe labeling was performed as described above; *in vitro* protein concentrations were normalized prior to probe labeling to match those for *in vivo* labeling. Click chemistry mediated attachment of a tetramethylrhodamine fluorophore, SDS-PAGE, and fluorescent gel analysis was carried out as described previously.[47] Protein loading in each gel lane was confirmed by Coomassie staining.

LC–MS Sample Preparation and Quantitative Analysis for *in Vitro* and *in Vivo* Probe-Labeled Samples and Global Unlabeled Samples. For probe labeled samples, following probe labeling, proteomes were treated with biotin-azide (36 μM), TCEP (2.5 mM), tris[(1-benzyl-1*H*-1,2,3-triazol-4-yl)methyl]amine (TBTA) (250 μM), and $CuSO_4$ (0.50 mM). The samples were vortexed and incubated at 24 °C for 1.5 h. Probe-labeled proteins were enriched on streptavidin resin, reduced with TCEP, and alkylated with IAM. Proteins were digested on-resin with trypsin, and the resulting peptides were collected for LC–MS analysis. Peptides identified by MS for global and probe-labeled samples were required to be at least six amino acids in length having a mass spectra generating function score of $\leq 1 \times 10^{-10}$, which corresponds to an FDR of <1%. For full details see the Supporting Information, including how sites of cysteine probe modification were determined.

Confocal Laser-Scanning Microscopy of *in Vivo* Probe-Labeled *Synechococcus* 7002. *In vivo* labeled *Synechococcus* 7002 cells (100 μL) and unlabeled cells (control; 100 μL) were probe-labeled and fixed with 3.7% formaldehyde in PBS, and then cells were washed 3× and permeabilized using 0.1% Triton X-100 in PBS. Next, cells were washed 3×, treated with AlexaFluor-488 *via* a Click-iT kit (Life Technologies), and then imaged by confocal laser-scanning microscopy. See the Supporting Information for full details.

Photophysiology. Chlorophyll fluorescence measurements were performed using pulse amplitude modulated fluorometry in a DUAL-PAM-100 (Walz GmbH) with a photodiode detector and RG665 filter. Samples were obtained from the CO_2-limited chemostat (−60 min), after 48 min of C-starvation (−12 min), and throughout the time-course after C-replenishment (0.5, 6, 12, 20, 30, 40, 52, 62 min). For full details and calculations see the Supporting Information.

Curation of Gene Product Functional Predictions. Automated function predictions for *Synechococcus* 7002 proteins were curated using information from the primary literature, databases, and automated pipeline. See the Supporting Information.

ASSOCIATED CONTENT

Supporting Information

The material is available free of charge *via* the Internet at http://pubs.acs.org.

AUTHOR INFORMATION

Corresponding Author

*E-mail: aaron.wright@pnnl.gov.

Notes

The authors declare no competing financial interest.

Data Availability: The mass spectrometry proteomics data have been deposited to the ProteomeXchange Consortium *via* the PRIDE partner repository with the data set identifier PXD000329.

ACKNOWLEDGMENTS

We thank B. Cravatt (The Scripps Research Institute) and E. Weerapana (Boston College) for providing biotin-TEV-Azide and related helpful discussions. This research was supported by the Genomic Science Program of the U.S. DOE-OBER and is a contribution of the PNNL Biofuels and Foundational Scientific Focus Areas. MS-based proteomic measurements used capabilities developed partially under the GSP Panomics project; MS-based measurements and microscopy were performed in the Environmental Molecular Sciences Laboratory, a national scientific user facility sponsored by OBER at PNNL.

REFERENCES

(1) Asada, K. (2006) Production and scavenging of reactive oxygen species in chloroplasts and their functions. *Plant Physiol. 141*, 391−396.

(2) Foyer, C. H., and Noctor, G. (2005) Redox homeostasis and antioxidant signaling: A metabolic interface between stress perception and physiological responses. *Plant Cell 17*, 1866−1875.

(3) Dietz, K. J., and Pfannschmidt, T. (2011) Novel regulators in photosynthetic redox control of plant metabolism and gene expression. *Plant Physiol. 155*, 1477−1485.

(4) Buchanan, B. B., and Balmer, Y. (2005) Redox regulation: A broadening horizon. *Annu. Rev. Plant Biol. 56*, 187−220.

(5) Yano, H., Wong, J. H., Lee, Y. M., Cho, M. J., and Buchanan, B. B. (2001) A strategy for the identification of proteins targeted by thioredoxin. *Proc. Natl. Acad. Sci. U.S.A. 98*, 4794−4799.

(6) Hishiya, S., Hatakeyama, W., Mizota, Y., Hosoya-Matsuda, N., Motohashi, K., Ikeuchi, M., and Hisabori, T. (2008) Binary reducing equivalent pathways using nadph-thioredoxin reductase and ferredoxin-thioredoxin reductase in the cyanobacterium *Synechocystis* sp. Strain pcc 6803. *Plant Cell Physiol. 49*, 11−18.

(7) Lindahl, M., and Florencio, F. J. (2003) Thioredoxin-linked processes in cyanobacteria are as numerous as in chloroplasts, but targets are different. *Proc. Natl. Acad. Sci. U.S.A. 100*, 16107−16112.

(8) Lindahl, M., and Kieselbach, T. (2009) Disulphide proteomes and interactions with thioredoxin on the track towards understanding redox regulation in chloroplasts and cyanobacteria. *J. Proteomics 72*, 416−438.

(9) Francisco, J., Florencio, F., Perez-Perez, M. E., Maury, L. L., Mata-Cabana, A., and Lindahl, M. (2006) The diversity and complexity of the cyanobacterial thioredoxin systems. *Photosynth. Res. 89*, 157−171.

(10) Montrichard, F., Alkhalfioui, F., Yano, H., Vensel, W. H., Hurkman, W. J., and Buchanan, B. B. (2009) Thioredoxin targets in plants: the first 30 years. *J. Proteomics 72*, 452−474.

(11) Lindahl, M., Mata-Cabana, A., and Kieselbach, T. (2011) The disulfide proteome and other reactive cysteine proteomes: analysis and functional significance. *Antioxid. Redox Signaling 14*, 2581−2642.

(12) Jones, D. P. (2008) Radical-free biology of oxidative stress. *Am. J. Physiol. Cell. Physiol. 295*, C849−C868.

(13) Held, J. M., and Gibson, B. W. (2012) Regulatory control or oxidative damage? Proteomic approaches to interrogate the role of cysteine oxidation status in biological processes, *Mol. Cell. Proteomics 11*, R111 013037.

(14) McDonagh, B., Padilla, C. A., Pedrajas, J. R., and Barcena, J. A. (2011) Biosynthetic and iron metabolism is regulated by thiol proteome changes dependent on glutaredoxin-2 and mitochondrial peroxiredoxin-1 in *Saccharomyces cerevisiae*. *J. Biol. Chem. 286*, 15565−15576.

(15) Fomenko, D. E., Xing, W., Adair, B. M., Thomas, D. J., and Gladyshev, V. N. (2007) High-throughput identification of catalytic redox-active cysteine residues. *Science 315*, 387−389.

(16) Cheng, Z., Zhang, J., Ballou, D. P., and Williams, C. H., Jr. (2011) Reactivity of thioredoxin as a protein thiol-disulfide oxidoreductase. *Chem. Rev. 111*, 5768−5783.

(17) Hansen, R. E., and Winther, J. R. (2009) An introduction to methods for analyzing thiols and disulfides: Reactions, reagents, and practical considerations. *Anal. Biochem. 394*, 147−158.

(18) Creighton, T. E. (1984) Disulfide bond formation in proteins. *Methods Enzymol. 107*, 305−329.

(19) Leonard, S. E., and Carroll, K. S. (2011) Chemical 'omics' approaches for understanding protein cysteine oxidation in biology. *Curr. Opin. Chem. Biol. 15*, 88−102.

(20) Leichert, L. I., and Jakob, U. (2004) Protein thiol modifications visualized in vivo. *PLoS Biol. 2*, e333.

(21) Delaunay, A., Isnard, A. D., and Toledano, M. B. (2000) H2O2 sensing through oxidation of the yap1 transcription factor. *EMBO J. 19*, 5157−5166.

(22) Shevela, D., Eaton-Rye, J. J., Shen, J. R., and Govindjee. (2012) Photosystem II and the unique role of bicarbonate: A historical perspective. *Biochim. Biophys. Acta Bioenerg. 1817*, 1134−1151.

(23) Laisk, A., Siebke, K., Gerst, U., Eichelmann, H., Oja, V., and Heber, U. (1991) Oscillations in photosynthesis are initiated and supported by imbalances in the supply of atp and nadph to the calvin cycle. *Planta 185*, 554−562.

(24) Gygi, S. P., Rist, B., Gerber, S. A., Turecek, F., Gelb, M. H., and Aebersold, R. (1999) Quantitative analysis of complex protein mixtures using isotope-coded affinity tags. *Nat. Biotechnol. 17*, 994−999.

(25) Weerapana, E., Wang, C., Simon, G. M., Richter, F., Khare, S., Dillon, M. B., Bachovchin, D. A., Mowen, K., Baker, D., and Cravatt, B. F. (2010) Quantitative reactivity profiling predicts functional cysteines in proteomes. *Nature 468*, 790−795.

(26) Jeffery, D. A., and Bogyo, M. (2003) Chemical proteomics and its application to drug discovery. *Curr. Opin. Biotechnol. 14*, 87−95.

(27) Speers, A. E., and Cravatt, B. F. (2004) Profiling enzyme activities in vivo using click chemistry methods. *Chem. Biol. 11*, 535−546.

(28) Smith, R. D., Anderson, G. A., Lipton, M. S., Pasa-Tolic, L., Shen, Y., Conrads, T. P., Veenstra, T. D., and Udseth, H. R. (2002) An accurate mass tag strategy for quantitative and high-throughput proteome measurements. *Proteomics 2*, 513−523.

(29) Rogers, L. K., Leinweber, B. L., and Smith, C. V. (2006) Detection of reversible protein thiol modifications in tissues. *Anal. Biochem. 358*, 171−184.

(30) Strasser, R., Tsimilli-Michael, M., and Srivastava, A. (2004) Analysis of the chlorophyll a fluorescence transient, in *Chlorophyll a Fluorescence* (Papageorgiou, G., and Govindjee, Eds.), pp 321−362, Springer, The Netherlands.

(31) Umena, Y., Kawakami, K., Shen, J.-R., and Kamiya, N. (2011) Crystal structure of oxygen-evolving photosystem II at a resolution of 1.9Å. *Nature 473*, 55−60.

(32) Wilson, A., Boulay, C., Wilde, A., Kerfeld, C. A., and Kirilovsky, D. (2007) Light-induced energy dissipation in iron-starved cyanobacteria: Roles of Ocp and IsiA proteins. *Plant Cell 19*, 656−672.

(33) Kinney, J. N., Axen, S. D., and Kerfeld, C. A. (2011) Comparative analysis of carboxysome shell proteins. *Photosynth. Res. 109*, 21−32.

(34) Wilson, A., Boulay, C., Wilde, A., Kerfeld, C., and Kirilovsky, D. (2007) Light induced energy dissipation in iron-starved cyanobacteria: Roles of Ocp and IsiA proteins. *Photosynth. Res. 91*, 312−312.

(35) Geigenberger, P. (2011) Regulation of starch biosynthesis in response to a fluctuating environment. *Plant Physiol. 155*, 1566−1577.

(36) Napolitano, M., Rubio, M. A., Santamaria-Gomez, J., Olmedo-Verd, E., Robinson, N. J., and Luque, I. (2012) Characterization of the response to zinc deficiency in the cyanobacterium *Anabaena* sp strain pcc 7120. *J. Bacteriol. 194*, 2426−2436.
(37) Shcolnick, S., Summerfield, T. C., Reytman, L., Sherman, L. A., and Keren, N. (2009) The mechanism of iron homeostasis in the unicellular cyanobacterium *Synechocystis* sp pcc 6803 and its relationship to oxidative stress. *Plant Physiol. 150*, 2045−2056.
(38) Oliveira, P., and Lindblad, P. (2009) Transcriptional regulation of the cyanobacterial bidirectional hox-hydrogenase. *Dalton Trans.*, 9990−9996.
(39) Stavrovskaya, E., Mironov, A., Rodionov, D., Dubchak, I., and Novichkov, P. (2012) Automated regulon content prediction and estimation of PWM quality. *Bioinformatics*, 322−325.
(40) Yamauchi, Y., Kaniya, Y., Kaneko, Y., and Hihara, Y. (2011) Physiological roles of the cyabrb transcriptional regulator pair sll0822 and sll0359 in *Synechocystis* sp. Strain pcc 6803. *J. Bacteriol. 193*, 3702−3709.
(41) Dominguez-Solis, J. R., He, Z., Lima, A., Ting, J., Buchanan, B. B., and Luan, S. (2008) A cyclophilin links redox and light signals to cysteine biosynthesis and stress responses in chloroplasts. *Proc. Natl. Acad. Sci. U.S.A. 105*, 16386−16391.
(42) Dietz, K. J. (2011) Peroxiredoxins in plants and cyanobacteria. *Antioxid. Redox Signaling 15*, 1129−1159.
(43) Mullineaux, C. W., and Allen, J. F. (1990) State-1-state-2 transitions in the cyanobacterium synechococcus 6301 are controlled by the redox state of electron carriers between photosystem-I and photosystem-II. *Photosynth. Res. 23*, 297−311.
(44) Bukhov, N., and Carpentier, R. (2004) Alternative photosystem I-driven electron transport routes: mechanisms and functions. *Photosynth. Res. 82*, 17−33.
(45) Ray, J. C. J., Tabor, J. J., and Igoshin, O. A. (2011) Non-transcriptional regulatory processes shape transcriptional network dynamics. *Nat. Rev. Microbiol. 9*, 817−828.
(46) Buchanan, B. B., Holmgren, A., Jacquot, J. P., and Scheibe, R. (2012) Fifty years in the thioredoxin field and a bountiful harvest. *Biochim. Biophys. Acta 1820*, 1822−1829.
(47) Ansong, C., Ortega, C., Payne, S. H., Haft, D. H., Chauvigne-Hines, L. M., Lewis, M. P., Ollodart, A. R., Purvine, S. O., Shukla, A. K., Fortuin, S., Smith, R. D., Adkins, J. N., Grundner, C., and Wright, A. T. (2013) Identification of widespread adenosine nucleotide binding in *Mycobacterium tuberculosis*. *Chem. Biol. 20*, 123−133.